

Dynamics after Interaction Quenches in One-Dimensional Fermionic Systems

Simone A. Hamerla^{1,*} and Götz S. Uhrig^{1,†}

¹ *Lehrstuhl für Theoretische Physik I, Technische Universität Dortmund,
Otto-Hahn Straße 4, 44221 Dortmund, Germany*

(Dated: July 10, 2012)

We show that the dynamics of quenches in one dimension far off equilibrium can be described by power laws, but with exponents differing from the fully renormalized ones at lowest energies. Instead they depend on the initial state and its excitation energy. Furthermore, we found that for quenches to strong interactions unexpected similarities between systems in one and in infinite dimensions occur, indicating the dominance of local processes.

PACS numbers: 05.70.Ln, 71.10.Pm, 67.85.-d, 71.10.Fd

In the last years, seminal experimental setups have been developed combining a very good decoupling of the quantum systems from their environment with a high degree of controllability of the system's parameters. This renders the observation of the temporal evolution of closed quantum systems for long times possible. Changing the internal parameters provides tools to investigate systems out of equilibrium. In optical lattices a change in the trapping potential and the external frequency is used to manipulate the internal parameters such as hopping and particle-particle interaction [1–4]. Furthermore, various pump-probe experiments based on ultrafast spectroscopy [5] have been developed [4].

These developments have triggered extensive theoretical studies of physics far from equilibrium, based on a large variety of analytical and numerical tools [3, 6–11, 13–15]. The goal is to qualitatively understand and to quantitatively describe the dynamics of quantum systems far from thermal equilibrium. How do such states evolve? Do they relax towards equilibrium? How does this happen and on which time scales?

These issues are relevant in all dimensions. But so far the one-dimensional (1D) case has attracted the greatest interest. On the one hand, this is because the 1D case is amenable to a larger variety of approaches. On the other hand, there are fascinating conceptual issues inherent to 1D systems: (i) All extended non-trivial integrable quantum systems are 1D and the existence of an exhaustive number of conserved quantities influences the dynamics strongly [16]. (ii) Gapless 1D systems are successfully described in the low-energy sector by free bosonic field theories [17–22]. Thus the question arises whether the same or similar bosonic field theories are also able to describe the nonequilibrium dynamics [23, 24]. This point is related to (i) because a free bosonic theory is integrable. Still, relaxation in local quantities due to dephasing may occur [25].

In this work we provide evidence that gapless bosonic field theories can indeed describe nonequilibrium dynamics in infinite 1D systems implying power laws. For the accessible times, the appropriate exponents are not the equilibrium exponents if the system is strongly quenched.

The effect goes beyond the substitution $\gamma \rightarrow 2\gamma(1 + \gamma)$ which appears in quenches of Luttinger liquids (LL) where γ is the equilibrium exponent [7, 13, 26]. Further, we argue that the power laws observed at short and moderate times remain meaningful for larger times if the macroscopic excitation energy $\Delta E/L$ (L : system size) induced by the quench is sufficiently large because $\Delta E/L$ cuts off the renormalization (RG) flow which would yield the equilibrium exponents at its fixed point. This is our first key result. Our second key result ensues from the comparison of the 1D dynamics to the one at infinite dimension where dynamic mean field theory (DMFT) is exact [3, 8, 11]. Much to our surprise strong qualitative similarities occur.

Quenches are an efficient way to realize states far from equilibrium [25]. Often, the interaction value is changed abruptly increasing it [7, 9–11, 13, 27] or decreasing it [15]. We focus on interactions which are suddenly switched on and consider Fermi seas as initial states.

Two generic fermionic lattice models are studied. The first are spinless fermions

$$H_{\text{NN}} = -J \sum_{\langle i,j \rangle} (\hat{c}_i^\dagger \hat{c}_j + \text{h.c.}) + U(t) \sum_i \hat{n}_i \hat{n}_{i+1} \quad (1)$$

with nearest-neighbor repulsion (NN), where \hat{c}_j^\dagger (\hat{c}_j) create (annihilate) a particle at site j and $\hat{n}_j = \hat{c}_j^\dagger \hat{c}_j$. The second is the Hubbard model comprising spin $\sigma = \uparrow, \downarrow$

$$H_{\text{Hu}} = -J \sum_{\langle i,j;\sigma \rangle} (\hat{c}_{i,\sigma}^\dagger \hat{c}_{j,\sigma} + \text{h.c.}) + U(t) \sum_i \hat{n}_{i,\uparrow} \hat{n}_{i,\downarrow} \quad (2)$$

and local repulsion. We study $U(t) = \Theta(t)U \geq 0$ and define the band width $W = 4J$ as energy scale. Below some quantities with spin σ are denoted; for the corresponding ones without spin σ is to be omitted.

The approach used is an expansion of the Heisenberg equations of motion for $\hat{c}_{j,\sigma}^\dagger$ in powers of the time t [13]. By commuting H after the quench recursively with $\hat{c}_{j,\sigma}^\dagger$ we obtain differential equations for the prefactors of the expansion of $\hat{c}_{j,\sigma}^\dagger(t)$ in monomials of $\hat{c}_{i,\sigma}^\dagger$ and \hat{c}_j at $t = 0$. The application of one commutation is a ‘loop’; up to

11 loops are realized. A conceptual asset is that the approach works for the infinite lattice by exploiting translational invariance, see Supplemental Material.

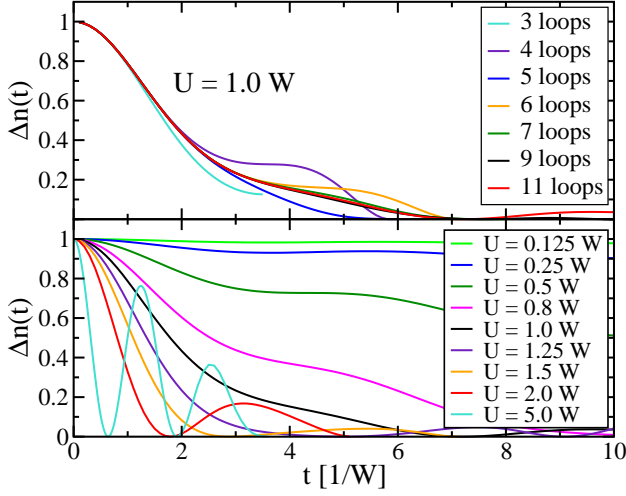


FIG. 1: (color online) Upper panel: Jump $\Delta n(t)$ for the half-filled Hubbard model for various loop numbers. Lower panel: $\Delta n(t)$ for increasing U (from top to bottom at small t) in 11 loops.

We focus on the momentum distribution $n_k(t) := \langle \hat{c}_{k,\sigma}^\dagger \hat{c}_{k,\sigma} \rangle(t)$ where k is the wave vector [13]. In particular we study the jump $\Delta n(t) := n_{k_F+0}(t) - n_{k_F-0}(t)$ at the Fermi vector k_F . In the initial Fermi sea $\Delta n(0) = 1$ holds. After the quench, Δn shows slow relaxation to zero [7, 13, 27] and coherent oscillations [23, 26]. The upper panel of Fig. 1 depicts the jumps for increasing number of loops for the half-filled Hubbard model. Good convergence is obtained for 11 loops up to about $t \approx 10/W$. The precise value up to which the data is reliable depends on the details. The lower panel of Fig. 1 displays the data for various values of U .

In Fig. 2 the jump $\Delta n(t)$ is shown for the spinless NN model. The data agrees very well with the data by Karrasch et al. in Fig. 1 of Ref. 23 obtained by time-dependent infinite-size DMRG. We compare our data to the analytic power law [13]

$$\Delta n(t) = \left[\frac{r_\rho^2}{r_\rho^2 + (2v_\rho t)^2} \right]^{\gamma_\rho(1+\gamma_\rho)} \left[\frac{r_\sigma^2}{r_\sigma^2 + (2v_\sigma t)^2} \right]^{\gamma_\sigma(1+\gamma_\sigma)} \quad (3)$$

where $\nu \in \{\rho, \sigma\}$ stands for charge (ρ) or spin (σ) channel. The parameters r_ν are length scales, v_ν velocities and γ_ν the exponents which read $\gamma_\nu = (K_\nu + K_\nu^{-1} - 2)/4$ as function of the K_ν value from bosonization. For the spinless case all quantities coincide $K = K_\rho = K_\sigma$, $r = r_\rho = r_\sigma$ and so on. The dashed lines in Fig. 2 use

$$K_{GS} = \pi/[2(\pi - \arccos(2U/W))] \quad (4a)$$

$$v_{GS} = \pi \sin(\arccos(2U/W))/[2 \arccos(2U/W)], \quad (4b)$$

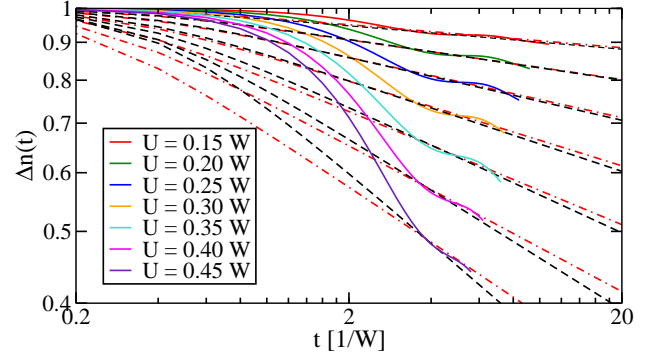


FIG. 2: (color online) Solid lines: $\Delta n(t)$ in the half-filled NN model for increasing U (from top to bottom) in 11 loops. Dashed lines: $\Delta n(t)$ as in Eq. (3) with the ground state (GS) exponents from Eq. (4). Dashed-dotted lines: $\Delta n(t)$ with the Fermi sea (FS) exponents from Eq. (5).

from Bethe ansatz [17, 28] reflecting the equilibrium excitations close to the ground state (GS). The cutoff length r is fitted and evolves from 0.4 and 0.6 on increasing U . The formulae are reasonable only up to $U = W/2$ where the system enters a gapped phase.

The dashed-dotted lines use the values [22]

$$K_{FS} = \sqrt{(\pi v_F - U)/(\pi v_F + 3U)} \quad (5a)$$

$$v_{FS} = (1/\pi) \sqrt{(\pi v_F + U)^2 - 4U^2} \quad (5b)$$

which result from bosonization around the Fermi sea (FS) [17, 18, 20, 21]. The fitted cutoff length r varies from 0.4 and 0.2 on rising U . The FS parameters characterize the LL Hamiltonian which describes bosonic modes in the vicinity of the FS, if processes not captured by the LL, e.g., the curvature of the dispersion, do not matter much. Then the FS exponents are surely relevant at short and moderate times when the system is still close to the FS. The GS parameters characterize the LL Hamiltonian of the bosonic modes close to the GS. Hence they are surely relevant for long times in equilibrium.

The FS formulae are reasonable only up to $U \approx W$ where v_{FS} vanishes at $U = \pi v_F$. For large U the effects of umklapp scattering and dispersion curvature hamper the bosonization approach.

Inspecting Fig. 2 we see that the microscopic model displays oscillations in $\Delta n(t)$ which are absent in Eq. (3). These oscillations can be ascribed to the momentum cutoff of the interaction in microscopic models [23, 26]. Otherwise, the power law (3) nicely describes the dynamics at moderate times in agreement with Ref. 23. It cannot be decided which of the two sets (GS and FS) fits better to the microscopic data, though the FS power law fits slightly better at $U \geq 0.4W$. The reasons are the small differences in K from (4) and (5) as long as $U < W/2$. This is accord with the closeness of the quenched NN system to equilibrium as measured by en-

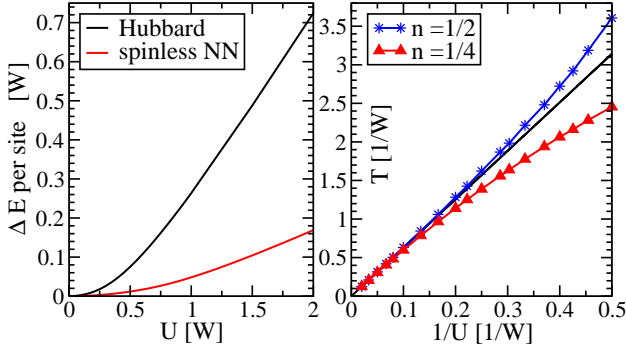


FIG. 3: (color online) Left panel: Energy expectation value of the Fermi sea relative to the ground state energy at half-filling for the Hubbard and the NN model. Right panel: Period of coherent oscillations in the strong interaction regime of the Hubbard model; n is the filling factor of one spin species.

ergy $\Delta E = \langle \text{FS} | H(t > 0) | \text{FS} \rangle - E_0$ which is excited in the system by the quench, see left panel of Fig. 3. The ground state energy E_0 results from Bethe ansatz [28, 29]. For the NN model ΔE stays very small up to $U = W/2$ where the gapped phase begins [28]. For the Hubbard model much larger energies are reached.

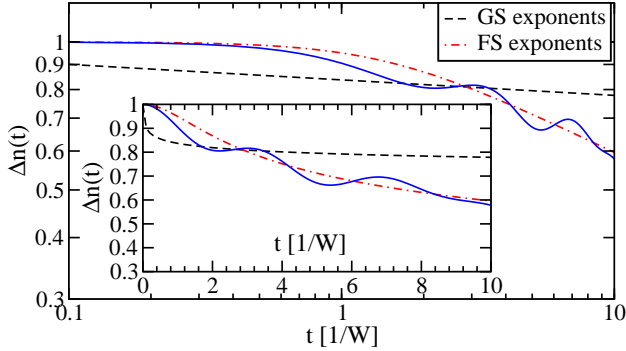


FIG. 4: (color online) Jump $\Delta n(t)$ for the Hubbard model at quarter-filling at $U = 0.8W$. Lines as in Fig. 2. For the GS exponents $r_\rho \approx 0.01$ is fitted; r_σ does not occur. For the FS exponents $r_\rho \approx 1$ and $r_\sigma \approx 0.6$ are fitted;

To distinguish between GS and FS exponents on the available time scales a model is needed where they differ significantly. The Hubbard model is a good candidate because of its ΔE values (Fig. 3) and because one of its K -values (K_σ for the spin channel) differs sizeably for GS ($K_{\sigma, \text{GS}} = 1$) and FS [20, 21]

$$K_{\rho, \text{FS}} = \sqrt{2\pi v_F / (2\pi v_F + 2U)} \quad (6a)$$

$$K_{\sigma, \text{FS}} = \sqrt{2\pi v_F / (2\pi v_F - 2U)} \quad (6b)$$

$$v_{\rho, \text{FS}} = v_F \sqrt{1 + U / (\pi v_F)} \quad (6c)$$

$$v_{\sigma, \text{FS}} = v_F \sqrt{1 - U / (\pi v_F)}. \quad (6d)$$

Indeed, the GS and the FS power laws differ significantly

in Fig. 4. The GS exponents result from Bethe ansatz [29, 30].

On the time scales studied, the FS power law captures the microscopic dynamics of $\Delta n(t)$ much better than the GS power law, see Supplemental Material for other U values. This supports our argument that the dynamics at short and moderate times can be described by a LL model with exponents relevant for the vicinity of the initial state, here the FS. This is the first key result.

Only the oscillations due to momentum cutoff [23, 26] are missed by the power law (3). For small values $U \lesssim 0.3W$ the differences between the GS and the FS power laws become small so that they are indistinguishable. For larger $U \gtrsim W$ the agreement between microscopic data and FS power laws deteriorates due the neglected physical processes (dispersion curvature, back scattering) in the LL.

The next intriguing question is what happens for longer times t ? To date this question cannot be answered definitely. Analytically, no RG theory for nonequilibrium physics exists. Numerically, no tools can treat long times far off equilibrium.

Karrasch et al. provide evidence by DMRG data for the NN model that the equilibrium LL is universal also in nonequilibrium in the sense that K_{GS} determines nonequilibrium power laws [23]. The underlying idea is that the relevant energy cutoff of the RG flow is $\propto 1/t$ so that for $t \rightarrow \infty$ the low-energy LL governs the physics.

We prefer the view point that there are two energy cutoffs $1/t$ and the excited energy $\Delta E/L$ because $\Delta E/L$ acts similar to a temperature smearing out smaller energy differences. Thus eventually $\max(1/t, \Delta E/L)$ should stop the flow. In this case, the initial high energy LL parameters relevant close to the FS flow very little if $\Delta E/L$ is large enough and the dynamics continues to be governed by the FS exponents. For instance, the flow of $K_{\sigma, \text{GS}}$ to its equilibrium value of 1 is logarithmically slow so that any substantial cutoff keeps it close to $K_{\sigma, \text{FS}}$. Since at present this issue cannot be decided further analytical and numerical work is called for: The regime $1/t < \Delta E/L$ for various values of $\Delta E/L$ would help to distinguish the two hypotheses.

Our second key result stems from the comparison of the 1D data with exact DMFT data for a Bethe lattice [3]. The common lore would expect a crucially distinct behavior due to the differing dimensionality and the integrability of the 1D Hubbard model [29]. The scattering in 1D is strongly restricted due to momentum conservation [17–19, 21, 22] while this conservation is irrelevant at internal vertices in DMFT [31]. Yet Fig. 7 shows qualitatively very similar results for larger values of U . While for $U \lesssim W$ differences prevail, the results for larger U , displaying coherent oscillations in $\Delta n(t)$ [3], agree up to the point that the minima appear at almost the same values. We conclude that these coherent oscillations are driven by local physics where the U term dominates. The

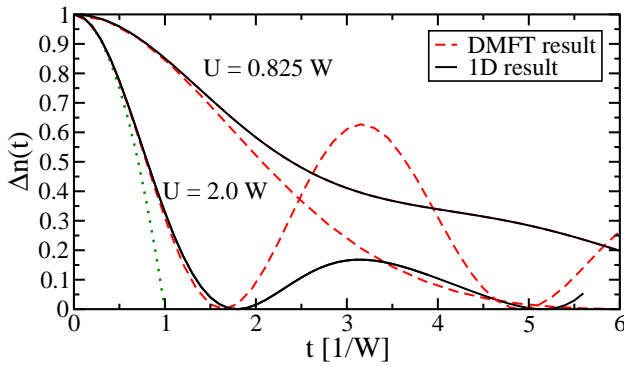


FIG. 5: (color online) Jump $\Delta n(t)$ for the half-filled Hubbard model in 1D (black, solid lines) and on the Bethe lattice (gray, dashed lines from Ref. [3]). Dotted line: Second order result $\Delta n = 1 - U^2 t^2 / 4$.

right panel in Fig. 3 supports this view: The period of the oscillations approaches $T = 2\pi/U$ of local Rabi oscillation between a singly and a doubly occupied site. The lattice acts as a damping bath. To stress that this is not simply an effect of the leading order in t the second order result $\Delta n(t) = 1 - U^2 n(1-n)t^2$ (n filling factor of one spin species) is included in Fig. 7.

Summarizing, we first showed that at short and moderate times the dynamics after interaction quenches in one dimension can be approximately described by a Luttinger liquid with parameters relevant around the initial states. For longer times, numerics is inconclusive, but we expect that for substantial excitation energy the Luttinger parameters hardly flow so that the relevant exponents remain close to the ones at short and moderate times: The equilibrium values are not reached.

Our second key result are unexpected similarities in the nonequilibrium dynamics after interaction quenches in Hubbard models in one dimension and on the infinitely branched Bethe lattice. In spite of fundamental differences in integrability and restriction in scattering both cases reveal damped coherent oscillations for larger values of U with almost identical frequency. This points towards a physics dominated by local processes.

Both these findings fundamentally enhance the understanding of nonequilibrium physics in one dimension which is an intensely studied focus these days. Further analysis, e.g., at longer times, is called for, but very difficult to reach to date.

We are indebted to A. Klümper and F. Essler for help in the evaluation of the Bethe ansatz results, to M. Eckstein, M. Kollar, and V. Meden for providing data, and to F. Becca, S. Kehrein, M. Kollar, V. Meden, M. Moeckel, and J. Stolze for inspiring discussions. We acknowledge support by the Studienstiftung des deutschen Volkes (SAH) and by the Mercator Stiftung (GSU).

* Electronic address: simone.hamerla@tu-dortmund.de

† Electronic address: goetz.uhrig@tu-dortmund.de

- [1] M. Greiner, O. Mandel, T. Esslinger, T. W. Hänsch, and I. Bloch, *Nature* **415**, 39 (2002).
- [2] M. Greiner, O. Mandel, T. W. Hänsch, and I. Bloch, *Nature* **419**, 39 (2002).
- [3] T. Kinoshita, T. Wenger, and D. S. Weiss, *Nature* **440**, 900 (2006).
- [4] I. Bloch, J. Dalibard, and W. Zwerger, *Rev. Mod. Phys.* **80**, 885 (2008).
- [5] L. Perfetti, P. A. Loukakos, M. Lisowski, U. Bovensiepen, H. Berger, S. Biermann, P. S. Cornaglia, A. Georges, and M. Wolf, *Phys. Rev. Lett.* **97**, 067402 (2006).
- [6] F. B. Anders and A. Schiller, *Phys. Rev. Lett.* **95**, 196801 (2005).
- [7] M. A. Cazalilla, *Phys. Rev. Lett.* **97**, 156403 (2006).
- [8] J. K. Freericks, V. M. Turkowski, and V. Zlatić, *Phys. Rev. Lett.* **97**, 266408 (2006).
- [9] C. Kollath, A. M. Läuchli, and E. Altman, *Phys. Rev. Lett.* **98**, 180601 (2007).
- [10] S. R. Manmana, S. Wessel, R. M. Noack, and A. Muramatsu, *Phys. Rev. Lett.* **98**, 210405 (2007).
- [11] M. Moeckel and S. Kehrein, *Phys. Rev. Lett.* **100**, 175702 (2008).
- [12] M. Eckstein, M. Kollar, and P. Werner, *Phys. Rev. Lett.* **103**, 056403 (2009).
- [13] G. S. Uhrig, *Phys. Rev. A* **80**, 061602(R) (2009).
- [14] T. Enss and J. Sirker, *New J. Phys.* **95**, 023008 (2012).
- [15] F. Goth and F. F. Assaad, *Phys. Rev. B* **85**, 085129 (2012).
- [16] M. Rigol, V. Dunjko, V. Yurovsky, and M. Olshanii, *Phys. Rev. Lett.* **98**, 050405 (2007).
- [17] A. Luther and I. Peschel, *Phys. Rev. B* **12**, 3908 (1975).
- [18] F. D. M. Haldane, *Phys. Rev. Lett.* **45**, 1358 (1980).
- [19] V. Meden and K. Schönhammer, *Phys. Rev. B* **46**, 15753 (1992).
- [20] K. Penc and J. Sólyom, *Phys. Rev. B* **47**, 6273 (1993).
- [21] J. Voit, *Rep. Prog. Phys.* **58**, 977 (1995).
- [22] E. Miranda, *Braz. J. Phys.* **33**, 3 (2003).
- [23] C. Karrasch, J. Rentrop, D. Schuricht, and V. Meden, 1205.2091.
- [24] E. Coira, F. Becca, and A. Parola, 1205.2967.
- [25] T. Barthel and U. Schollwöck, *Phys. Rev. Lett.* **100**, 100601 (2008).
- [26] J. Rentrop, D. Schuricht, and V. Meden, *New J. Phys.* p. 1203.0932.
- [27] B. Dóra, M. Haque, and G. Zaránd, *Phys. Rev. Lett.* **106**, 156406 (2011).
- [28] C. N. Yang and C. P. Yang, *Phys. Rev.* **150**, 321 and 327 (1966).
- [29] F. H. L. Essler, H. Frahm, F. Göhmann, A. Klümper, and V. E. Korepin, *The One-Dimensional Hubbard Model* (Cambridge University Press, UK, 2005).
- [30] H. J. Schulz, *Phys. Rev. Lett.* **64**, 2831 (1990).
- [31] E. Müller-Hartmann, *Z. Phys. B* **74**, 507 (1989).

SUPPLEMENTAL MATERIAL

TECHNICALITIES

We are interested in momentum distributions after interaction quenches. They can be computed by Fourier transformation from the one-particle equal time propagators

$$G(\vec{r}, t) = \langle \text{FS} | \hat{c}(\vec{r}, t) \hat{c}^\dagger(0, t) | \text{FS} \rangle \quad (7)$$

where the expectation value is taken with respect to the noninteracting Fermi sea $|\text{FS}\rangle$ which represents the initial state before the quench. The \vec{r} stands for a site on the lattice under study, here a chain in one dimension (1D). The time-dependent operators \hat{c} and \hat{c}^\dagger are represented by the following ansatz

$$\hat{c}^\dagger(\vec{r}, t) = \hat{T}_\vec{r}^\dagger + \hat{T}_\vec{r}^\dagger \left(\hat{T}^\dagger \hat{L}^\dagger \right)_\vec{r} + \dots \quad (8)$$

where \hat{T}^\dagger (\hat{L}^\dagger) denote various superpositions of particle (hole) creation operators. For instance, the single particle creation \hat{T}^\dagger is given as

$$\hat{T}_\vec{r}^\dagger = \sum_{|\vec{\delta}| \lesssim v_{\text{max}} t} \sum_{\sigma} h_0(\vec{\delta}, t) \hat{c}_{\vec{r}+\vec{\delta}, \sigma}^\dagger \quad (9)$$

with time-dependent prefactors $h_0(\vec{\delta}, t)$. The possible shift $\vec{\delta}$ which occurs is given by the maximal velocity v_{max} in the sense of the Lieb-Robinson theorem [1, 2].

To calculate the time dependence of the prefactors we use the Heisenberg equation $\partial_t \hat{A}(\vec{r}, t) = i [\hat{H}, \hat{A}(\vec{r}, t)]$ for the time derivative of an operator \hat{A} . On calculating the commutator $[\hat{H}, \hat{c}^\dagger(\vec{r}, t)]$ we encounter two cases. The commutation of the noninteracting part of the Hamiltonian \hat{H}_0 leads to a shift of the fermionic operators in space, whereas the commutation with the interaction term \hat{H}_{int} may additionally create or annihilate particle-hole pairs $(\hat{T}^\dagger \hat{L}^\dagger)$. Iterating this process then leads to the ansatz (8). With each commutation more terms with higher number of particles involved are created. Thus the amount of terms grows exponentially: At 11 loops we deal with up to $5 \cdot 10^5$ monomials in the Hubbard model and a set of differential equations with about $2 \cdot 10^7$ terms on the right hand side. In the spinless model with nearest-neighbor repulsion, we cope with up to $5 \cdot 10^5$ monomials and a set of differential equations with $7 \cdot 10^6$ terms on the right hand side.

The differential equations of the prefactors can be solved numerically with the initial conditions $h_0(0, 0) = 1$ and $h_i(\vec{r}, t) = 0 \forall i \neq 0$. Because each commutation comprises one order in time t a calculation with n commutations provides results for $\hat{c}^\dagger(t)$ which are exact up to order t^n . We stress, however, that we do not use a series

expansion in t but solve the (truncated) set of differential equations numerically.

Due to the proliferating number of additional terms arising within the calculation we have to restrict ourselves to a finite number of commutations. As terms appearing during the last commutation for the first time lead to an overestimation of the weight loss for the one particle terms, we omit them to improve the convergence. A calculation with n commutations performed in this way is called an n -loop calculation.

DYNAMICS IN THE HUBBARD CHAIN

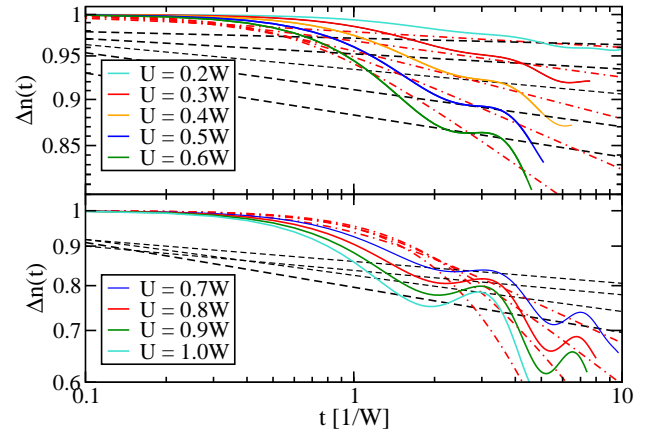


FIG. 6: (color online) Solid lines: $\Delta n(t)$ for the Hubbard model at quarter-filling for various values of U . Dashed lines: $\Delta n(t)$ given by the ground state (GS) exponents. Dashed-dotted lines: $\Delta n(t)$ calculated with the Fermi sea (FS) exponents.

Figure 6 shows the jump $\Delta n(t)$ of the momentum distribution at the Fermi vector for the Hubbard model at quarter-filling. We compare the data for the microscopic model to the power laws for Luttinger liquids with two different sets of exponents: The ground state (GS) exponents are taken from exact results; the Fermi sea (FS) exponents are taken from bosonization around the Fermi sea. As can be seen in the upper panel, the curves for the FS and the GS power law behave very similarly for small $U \lesssim 0.3W$. For larger values of U the time evolution of the jump is well described by the FS power law while the GS exponents do not fit the slope.

At $U = 1.0W$ the agreement worsens, which is explained by the breakdown of the Luttinger liquid description in terms of bosonic modes without interaction due to neglected scattering processes such as back scattering and umklapp scattering and due to the neglected curvature of the single-particle dispersion.

COMPARISON TO $\Delta n(t)$ ON THE BETHE LATTICE

Comparing the 1D results with the results for the Bethe lattice with infinite coordination number obtained from dynamic mean field theory (DMFT) [3], the curves show a surprisingly good agreement for larger values of the interaction U . As can be seen from the upper panel of Fig. 7, the curves for small U only agree for very small times in the leading quadratic order in t . For $U > W$ the DMFT and the 1D curves agree qualitatively. Their minima appear even quantitatively at about the same times.

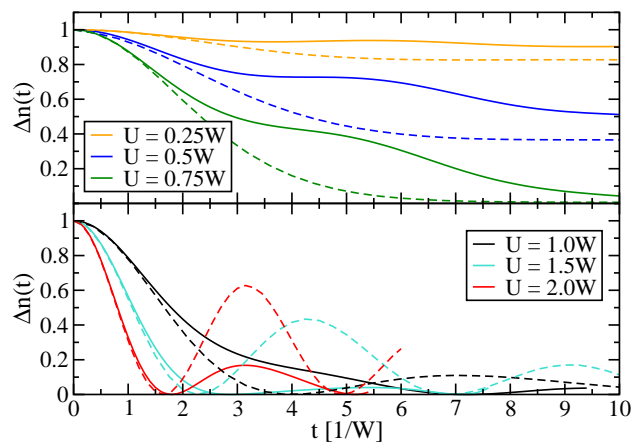


FIG. 7: (color online) Jump $\Delta n(t)$ for the half-filled 1D Hubbard model for various values of the interaction U . Solid lines: $\Delta n(t)$ for the 1D Hubbard model in 11 loops. Dashed lines: DMFT data for the Bethe lattice taken from Ref. [3]

* Electronic address: simone.hamerla@tu-dortmund.de

† Electronic address: goetz.uhrig@tu-dortmund.de

- [1] E. H. Lieb and D. W. Robinson, Commun. Math. Phys. **28**, 251 (1972).
- [2] P. Calabrese and J. Cardy, Phys. Rev. Lett. **96**, 136801 (2006).
- [3] M. Eckstein, M. Kollar, and P. Werner, Phys. Rev. Lett. **103**, 056403 (2009).